Virchows Archiv A Pathol Anat Histopathol (1988) 412:499–513

Virchows Archiv A
Pathological Anatomy and Histopathology

Alveolar soft part sarcoma

An immunohistochemical, cytologic and electron-microscopic study and a quantitative DNA analysis

S. Persson [1], J-S. Willems [2], L.-G. Kindblom [1], and L. Angervall [1]

[1] Department of Pathology, Sahlgren Hospital, Gothenburg University, S-41345 Göteborg, Sweden
[2] Karolinska Hospital, Stockholm, Sweden

Summary. The type, differentiation and histogenesis of the tumor cells of alveolar soft part sarcoma (ASPS) have been analyzed in a series of ten cases by a light-microscopic, ultrastructural, immunohistochemical and cytologic investigation and quantitative DNA analysis. Four tumors deviated from ordinary ASPS: three were wholly or partly of the so-called pleomorphic variant of ASPS and a fourth tumor showed calcifications of the psammoma body type. The ultrastructural findings and immunohistochemical demonstration of desmin supported the hypothesis of a rhabdomyomatous differentiation and gave no support to epithelial (negative immunoreactions for cytokeratins, epithelial membrane antigen, HMFG-1 and -2, tissue polypeptide antigen (TPA)) or neuroectodermal (negative for S-100 protein, glial fibrillary acidic protein, neurofilaments) differentiation. The negative immunoreactions for vimentin and myoglobin and the positive reaction for neuron specific enolase (NSE) do not exclude a rhabdomyomatous differentiation since in rhabdomyosarcomas the undifferentiated rhabdomyoblasts generally contain vimentin and the differentiated tumor cells contain myoglobin and rhabdomyosarcoma has previously been reported as being positive for NSE. The production of external lamina material peripherally in the tumor cell nests and around vessels in the vascular septa was demonstrated both ultrastructurally and by immunohistochemistry using antibodies against collagen IV and laminin. The cytologic appearance in smears obtained by fine-needle aspiration from a case of the pleomorphic variant showed some resemblance to that of a carcinoma. The seven tumors with an ordinary cell appearance were found to show a diploid DNA-distribution at a quantitative analysis performed on paraffin sections, while the three tumors wholly or partly of the pleomorphic type showed an additional tetraploid peak.

Key words: Alveolar soft part sarcoma – Cytology – Electron microscopy – Immunohistochemistry – DNA analysis

Offprint requests to: S. Persson

Introduction

Alveolar soft part sarcoma, (ASPS), named by Christopherson et al. (1952) is a rare soft tissue sarcoma with a characteristic light-microscopic appearance, but with an incompletely understood histogenesis. Ultrastructural findings of crystalline structures resembling those found in benign rhabdomyoma have been considered to support a rhabdomyomatous differentiation (Fisher and Reidbord 1971), and other findings of secretory-like granules, myelin sheaths and myelinated axons have supported a neural crest origin and its close relation to paraganglioma (Welsh et al. 1972; Unni and Soule 1975; Mathew 1982). Recently immunohistochemical techniques have been applied in order to shed light on the histogenesis of ASPS. The findings of Mukai et al. (1983, 1986) of a positivity for desmin, actin and Z-protein in three cases using polyclonal antibodies indicated a rhabdomyoblastic differentiation of ASPS. However, they found no positivity for myoglobin using polyclonal antibodies. Their study gave no support to a neural crest origin. The ultrastructural appearance of the characteristic rhomboid crystals of ASPS, first described ultrastructurally by Shipkey et al. (1964), was considered by DeSchryver-Kecskemeti et al. (1982) to resemble renin granules in human renal juxtaglomerular cells and they raised

the possibility that ASPS represents a variant of angioreninoma. An immunohistochemical study, utilizing a polyclonal renin-antibody, performed in four cases gave support to this theory (DeSchryver-Kecskemeti et al. 1982). Mukai et al. (1983) could not confirm the finding of renin, utilizing both immunohistochemical and biochemical analysis. There are also conflicting results when it comes to the expression of intermediate filaments in ASPS. Mukai et al. (1986) found vimentin positivity in all three cases studied, while Altmannsberger et al. (1986) only found focal positivity in one of two cases studied. Romdhane et al. (1985) reported cytokeratin-positivity in one case, using a monoclonal antibody, while Mukai et al. (1986) found no positivity using another monoclonal anticytokeratin antibody. Romdhane et al. also found a positivity for neuron-specific enolase (NSE), not found by Mukai et al.

In general the ultimate prognosis for patients with ASPS is rather poor, although metastases may appear very late in the course and prolonged survival can be seen even after metastases have developed (Enzinger and Weiss 1983). It has not been possible to correlate the variable course of ASPS to morphologic findings and there is no knowledge of the extremely rare pleomorphic variant (Christopherson et al. 1952; Enzinger and Weiss 1983; Evans 1985) in terms of prognosis. No quantitative DNA analysis of ASPS has been reported so far.

In this article a correlative ultrastructural and immunohistochemical analysis of ten cases of ASPS is presented in order to investigate the type and differentiation of the tumor cells. One of the cases represents the pleomorphic variant of ASPS and two others included pleomorphic areas. The investigation also includes a quantitative DNA analysis of the ten tumors and describes the cytologic appearance in smears from preoperative fine needle aspiration in one case of pleomorphic ASPS.

Material and methods

Nine cases of alveolar soft part sarcoma were obtained from our files at the Department of Pathology, Sahlgren Hospital, Gothenburg University, Sweden, and one case from the Department of Pathology, Karolinska Hospital, Stockholm, Sweden. Clinical data were obtained from clinical records.

Five micron sections were cut from the paraffin blocks and stained with the van Gieson trichrome staining and with hematoxylin-eosin. The PAS method with and without pretreatment of sections with diastase (E. Merck, Darmstadt, FRG) was used for studying the PAS-positive and diastase-resistant inclusions and glycogen. Silver impregnation according to Grimelius was performed in all cases. The mitotic activity was estimated by counting the number of mitoses in 30 random high-power fields (objective × 40, ocular × 10). After measuring the area of the visual field the mitotic activity per mm^2 could be estimated.

From case no 10 fine-needle aspirations were taken preoperatively from both a lung metastasis (through transthoracic aspiration) and from the primary tumor in the right thigh discovered 8 years later. Some of the smears were air-dried for May-Grünwald-Giemsa staining, while others were fixed in 95% methanol prior to Papanicolaou staining.

In one of the cases (case 10) small pieces of tissue fixed in 3% glutaraldehyde were available for electron microscopy. These pieces were washed in 0.1 M sodium cacodylate buffer, postfixed with 1% osmium tetroxide for 1 h, thereafter dehydrated in ethanol and embedded in epoxy resin. In two of the cases (cases 1 and 4) material fixed in 4% formaldehyde was

Table 1. Antisera used

Antibody		Antibody type	Concentration
Anti-Vimentin V9[a]		M	1/100[1]
Anti-Desmin 33[b]		M	1/40
Anti-Actin N350[c]		M	1/400
Anti-Myoglobin MG-1[d]		M	1/40[1]
Anti-Cytokeratins	CAM 5.2[e]	M	1/4
	AE1/AE3[f]	M	1/600
	PKK1[g]	M	1/100
	2080[b]	M	1/25
	A575[a]	P	1/500
	Z622[a]	P	1/400
	1084[d]	P	1/400
Epithelial membrane markers			
Anti-EMA[a]		M	1/100
Anti-HMFG-1[h]		M	1/25
Anti-HMFG-2[h]		M	1/25
Anti-TPA[i]		P	1/5[2]
Anti-FVIII-RAG[a]		P	1/500
Anti-S-100 protein[j]		P	1/2000[1]
Anti-Neurofilament[k]		M	1/4[1]
Anti-Glial fibrillary acidic-protein (GFAP)[a]		P	1/250
Anti-Neuron specific enolase (NSE)*		P	1/500[1]
Anti-Laminin[m]		P	1/1000
Anti-Collagen IV[m]		P	1/300

M = Monoclonal; *P* = Polyclonal

[1] only without trypsination
[2] only with trypsination

[a] Dako Corp., Santa Barbara, USA
[b] Monosan, Nistelrode, Holland
[c] Amersham, Amersham, Buckinghamshire, UK
[d] Bio-Yeda, Rehovot, Israel
[e] Becton Dickinson, CA, USA
[f] Hybritech, San Diego, CA, USA
[g] Labsystems, Helsinki, Finland
[h] Seward Lab, Bedford, UK
[i] Sangtec, Bromma, Sweden
[j] Haglid, Dept of Histology, University of Göteborg, Sweden
[k] MILAB, Malmö, Sweden
[l] BioGenex, Dublin, CA, USA
[m] Gift from L and I Risteli, University of Oulu, Finland

Table 2

Case number	Age (years)	Sex	Tumor site	Clinical data of 10 patients with ASPS		Follow-up
				Tumor size (cm)	Treatment of primary tumor	
1	22	Male	Intramuscular, left gluteal region	6 × 4	Local excision	Lung metastases after 2 years, dead with metastases after 5 years
2	33	Male	Intramuscular, left thigh	5 × 6	Local excision	Dead after 9 years with metastases to lung and brain.
3	29	Female	Recto-vaginal septum	6 × 5	Local excision	Local recurrence after 3 years, dead after 8 years with multiple skeletal metastases
4	19	Female	Intramuscular, right rectus muscle	1 × 2	Local excision	Alive and well after 6 years
5	22	Female	Intramuscular, right leg	7 × 3.5	Local excision	Alive and well after 24 years
6	15	Female	Intramuscular, right upper arm	5 × 5	local excision	Dead after 23 years with metastases to lung, heart and brain
7	7	Female	Intramuscular, left pectoral muscle	1 × 2	Local excision	
8	36	Male	Intramuscular, left leg	5 × 5	Local excision followed by amputation	Metastases to fibula and tibia at primary diagnosis, alive and well after 11 years
9	27	Male	Intramuscular, right gluteal	8 × 7 × 6	Local excision followed by chemotherapy	Dead after 1 year with metastases to lung and brain
10	26	Female	Intramuscular, right leg	6 × 6	Excision of a lung metastasis. The primary tumor and multiple lung metastases diagnosed and excised after 8 years	Alive and well after 10 years

available. Small pieces of this tissue were rinsed in buffer for 24 h and then processed as described above. In seven cases only paraffin-embedded material was available. Small pieces of tumor tissue were cut from selected areas of the paraffin blocks and were thereafter reprocessed for electron microscopy (Seidal and Kindblom 1984; Widéhn and Kindblom 1987). One micron thick sections were stained with toluidine blue and ultrathin sections cut on a LKB Ultrotome III were contrast stained with uranylacetate and lead citrate and examined under a Philips electron microscope 400.

The avidin-biotin-complex (ABC) method (Hsu et al. 1981) was applied to formalin-fixed and paraffin-embedded tissues. Prior to staining the paraffin sections were deparaffinized in xylene with and without subsequent digestion with 0.05% trypsin (Type III-S, Sigma Chemical Company, St. Louis, USA) for 20 min in 37° C. All sections were then treated with 0.5% H_2O_2 in methanol in order to reduce endogenous peroxidase activity. The ABC-method was performed with the Vectastain® ABC-kits (Vectastain, Vector labs, Burlingame, CA, USA) according to the instructions except for a prolonged incubation time for the primary antisera (16 h at 4 °C). The end products were visualized by treating the sections with a freshly made solution of 0.05% diaminobenzidine hydrochloride with 0.02% H_2O_2 in Tris buffered saline. The primary antisera used and their concentrations are given in Table 1.

Normal skin, including connective tissue and vessels, smooth and striated muscle, squamous carcinoma, ductal breast carcinoma, colon carcinoma and teratoma of ovary with glial tissue were used as control tissues for the immunohistochemical analyses as well as normal tissues surrounding the tumors.

One representative paraffin block was chosen from all ten of the tumors; from this consecutive sections were made for hematoxylin-eosin and Feulgen staining. After Feulgen-hydrolysis, performed at 22° C in 5N HCl for 60 min, nuclear DNA was measured at 546 nm in a scanning microspectrophotometer (Caspersson, 1979, 1980). In each section the nuclear absorption of 50 tumor cells was measured. As an internal staining control of the normal diploid value, the absorption of 25 to 30 nuclei from fibroblasts or endothelial cells in tissue adjacent to the tumor was measured. The mean DNA value of the control cells was determined in order to define a diploid standard (2 c). The DNA content of the tumor stemline, the modal value, was calculated for each tumor and expressed in relative units. However, three additional variables were registred: 1. the percentage of tumor cells exceeding the modal peak, determined graphically 2. the percentage of tumor cells exceeding the arbitrarily set upper limit of the diploid range at 2.5 c 3. the percentage of tumor cells exceeding the 90th percentile of DNA values of the control cells. In one case (case 8) where the histopathologic picture was not uniform comparative measurements of DNA were made in areas of both ordinary and pleomorphic appearance. In case 10, which was wholly of the pleomorphic

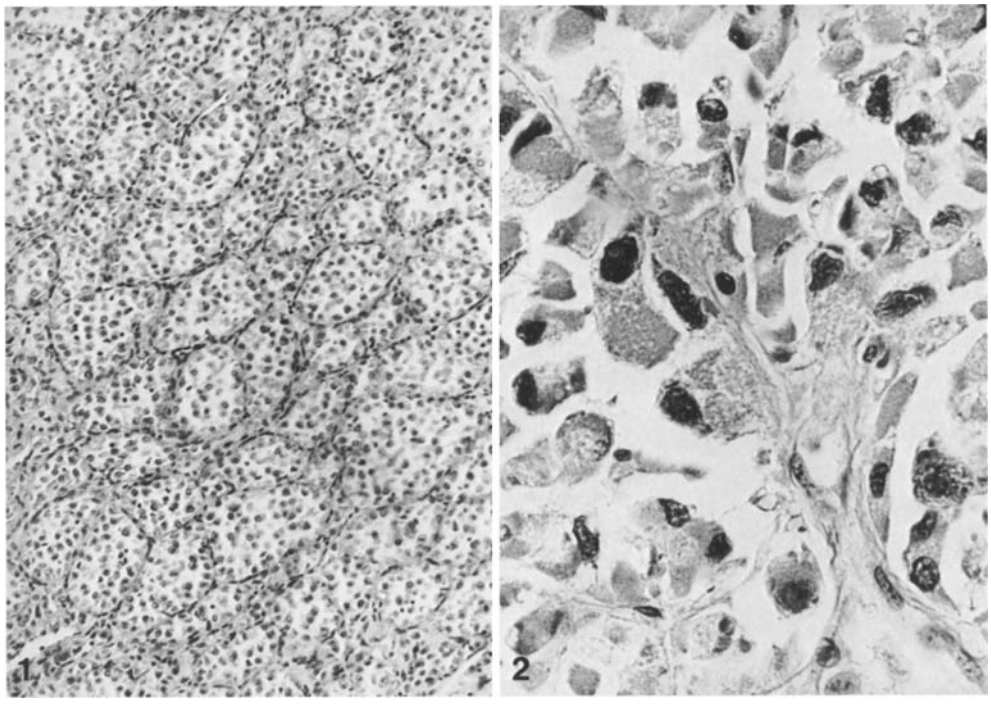

Fig. 1. Typical arrangement of tumor cells in alveolar and nest-like formations giving the tumor an organoid appearance. H & E, ×80

Fig. 2. Tumor area (case 10) showing a prominent cell and nuclear polymorphism. H & E, ×480

variant, the most pleomorphic and bizarre areas were compared with less pleomorphic areas. In this case the DNA content of the primary tumor and two consecutive lung metastases was also determined. Furthermore, comparison of measurements of tumor nuclei in paraffin sections and air-dried smears from fine-needle aspirates of the primary tumor was performed in this case, after destaining the May-Grünewald-Giemsa stain in methanol and subsequent Feulgen-hydrolysis as described above.

Results

Data on the age and sex of the patients, tumor site and size, given treatment and follow-up are summarized in Table 2.

Light microscopic appearance

All the tumors showed a similar growth pattern, characterized by dense fibrous septa dividing them into compartments of varying size. These compartments were further divided into distinct solid nests of tumor cells or alveolar formations of fairly uniform size, giving an organoid character (Fig. 1). The tumor cells were large and mostly showed little or moderate variation in size and shape and contained one or sometimes two, usually vesicular nuclei with a prominent nucleolus. In all cases the abundant eosinophilic and granular cytoplasm contained PAS-positive and diastase-resistent material, which was granular in most cells, but also crystalline and rod-shaped in a varying number of tumor cells. One of the tumors (case 10) and parts of two others (cases 3 and 8) differed by exhibiting polymorphic tumor cells often with multiple hyperchromatic nuclei (Fig. 2) and included atypical mitotic figures. The estimated mitotic activity was less than $1/mm^2$ in all tumors, including the tumors which were partly or predominantly of the pleomorphic type. Areas with calcifications partly of the so-called psammoma body type (Fig. 3) were a prominent feature of one tumor (case 1). The abundance of vessels in the delicate septa which divided the cell nests and alveolar formations was a characteristic finding in all cases. Often small tumor nodules were seen protruding into the lumen of larger thin-walled vessels, i.e. intravascular tumor growth. All tumors were intramuscular, showed a restricted infiltration and lacked encapsulation, although a fibrous coat, often containing large vessels, mostly of the venous type, often separated the tumor from the muscle tissue. There were areas of necrosis and bleeding in most cases. No positivity was seen in the tumor cells using the Grimelius silver impregnation method.

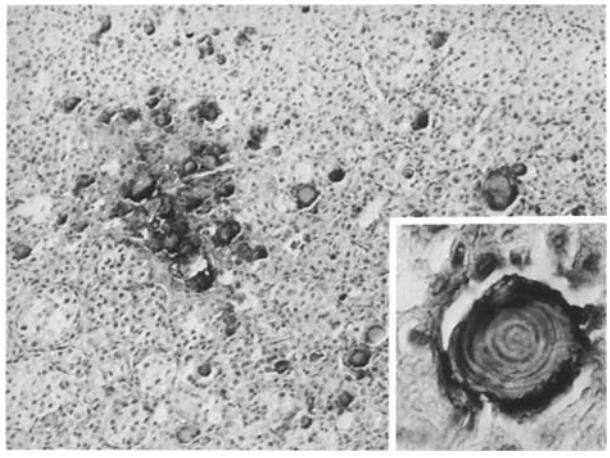

Fig. 3. Tumor area with numerous psammoma bodies. H & E, ×60, insertion ×450

Cytology

The fine needle aspiration smears (Fig. 4) from one of the cases (case 10) of the pleomorphic variant were dominated by tumor cell clusters filling out the mazes of a prominent vascular net work. In addition small aggregates of up to a dozen tumor cells, free lying tumor cells and capillary meshworks devoid of most of the tumor cells could were seen. The tumor cells were large, round to polygonal with a either a pale-staining, ill-defined cytoplasm containing numerous small round vacuoles or a dense, darker-staining cytoplasm with sharply delineated cell border. Most tumor cells contained a single nucleus, although there were bi- or multinucleated tumor cells. The nuclei were rounded, hyperchromatic and varied in size. In Papanicolaou-stained smears they showed a coarse chromatin pattern with conspicuous chromocenters, nuclear grooves and prominent nucleoli. There were numerous intranuclear cytoplasmic inclusions. Many such free-lying tumor cells were stripped of their cytoplasm. Such nuclei were often seen clumped together in groups of four or more. In May-Grünwald-Giemsa stained smears, the often spindle-shaped endothelial cells were found enveloped by a pink-staining fine fibrillary collagen matrix. The aspirated material from the lung metastasis was scant and consisted entirely of large tumor cells rich in cytoplasm as described above.

Electron microscopic appearance

The mostly rounded or polygonal tumor cells revealed an abundant cytoplasm and usually contained a single, rounded nucleus with smooth or indented outlines (Fig. 5a, b). The nuclei showed a finely dispersed chromatin with a very thin zone of condensed heterochromatin beneath the nuclear envelope and a single large, reticular nucleolus (Fig. 5a, b). In one case intranuclear glycogen deposits were found (Fig. 5b). The cytoplasm was

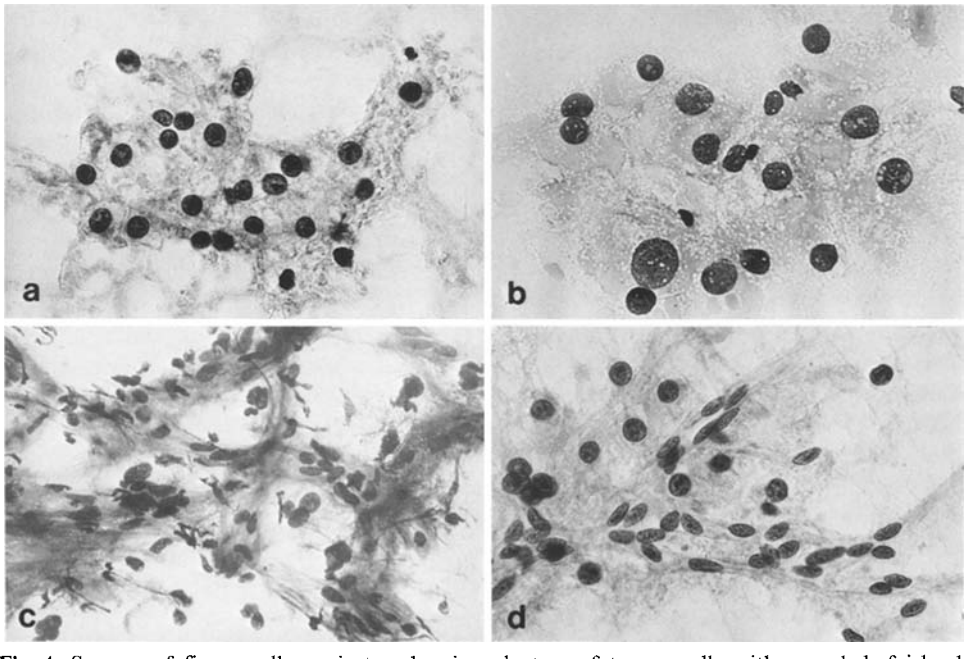

Fig. 4. Smears of fine needle aspirates showing clusters of tumor cells with rounded, fairly dense nuclei of varying size and with prominent nucleoli. The abundant cytoplasm is pale and ill-defined (**a** and **b**). Scattered tumor cells enclosed within a prominent capillary network (**c** and **d**). **a** and **c**, Papanicolou stain ×320, **b** and **d** May-Grünwald-Giemsa stain ×320

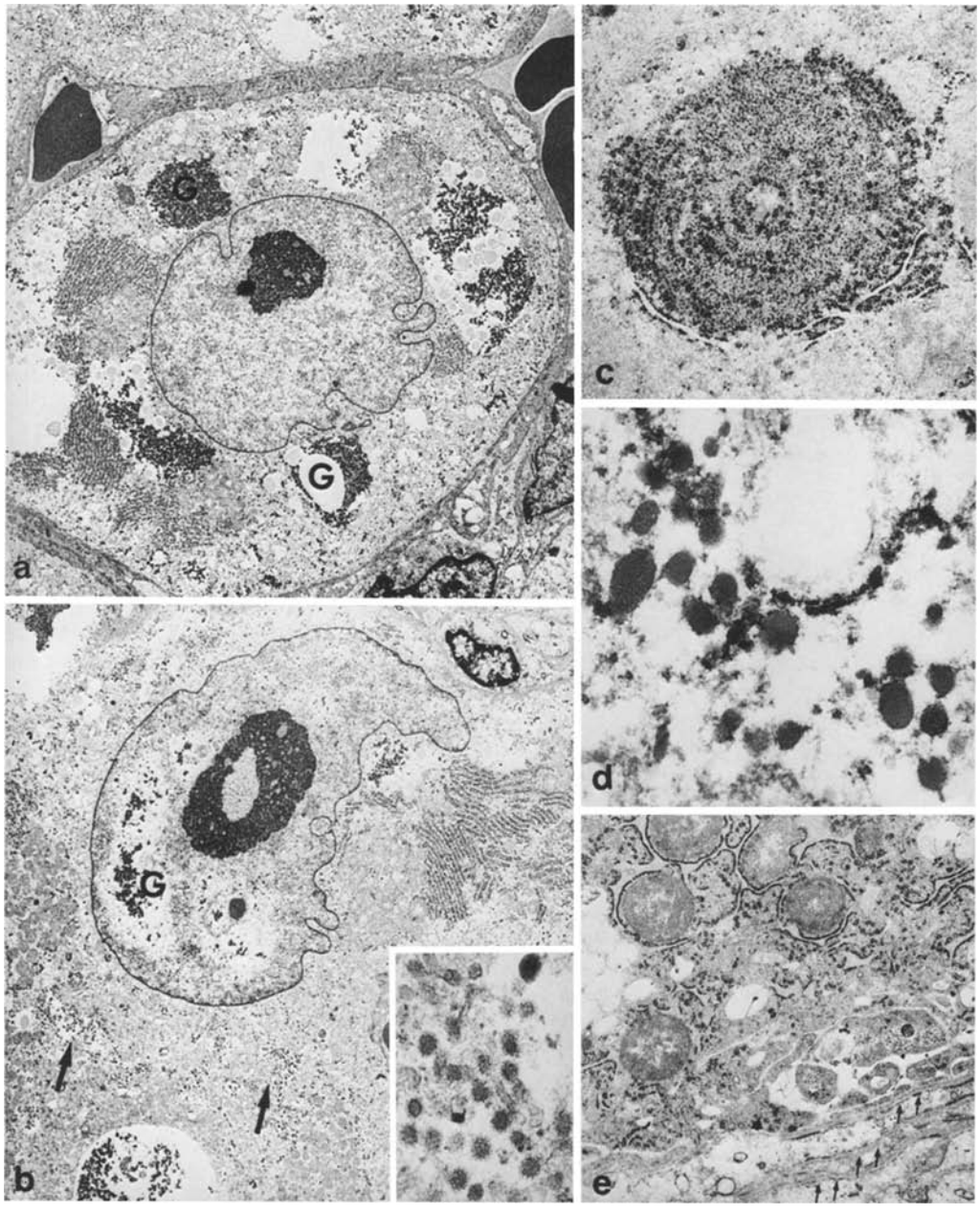

Fig. 5a and **b**. Rounded tumor cells with a single slightly indented nucleus with evenly dispersed chromatin and a prominent nucleolus. The cytoplasm shows abundant and focally distributed RER, mitochondria and glycogen (**a**). There are also some intranuclear glycogen deposits (**b**). Virus-like particles are marked with arrows in **b** and a magnification of these is inserted. **c** A characteristic ribosome-lamella complex. **d** Dense rounded, intracytoplasmic granules. **e** Rounded mitochondria enveloped by RER. The cytoplasmic membranes are lined by an external lamina (*arrows*). **a** ×2,960; **b** ×3,830, *insert* ×33,400; **c** ×13,900; **d** ×23,200; **e** ×10,80

characterized by a peculiarly organized distribution of the organelles; some parts of the cytoplasm were filled with mitochondria, other parts by rough endoplasmic reticulum (RER) and the perinuclear area often contained a well deliniated Golgi zone (Fig. 5b). A prominent feature of the RER was the formation of tightly packed narrow arrays and the frequent occurrence of ribosome-lamella complexes and concentric membranous bodies (Fig. 5c). RER was also seen to envelop groups of mitochondria (Fig. 5e). Occasionally segments of dilated RER filled with a dense, finely granular material were seen. The smooth endoplasmic reticulum was usually sparse. Occasionally it was dilated and filled with an internal material which formed structures of the size and shape and stain-

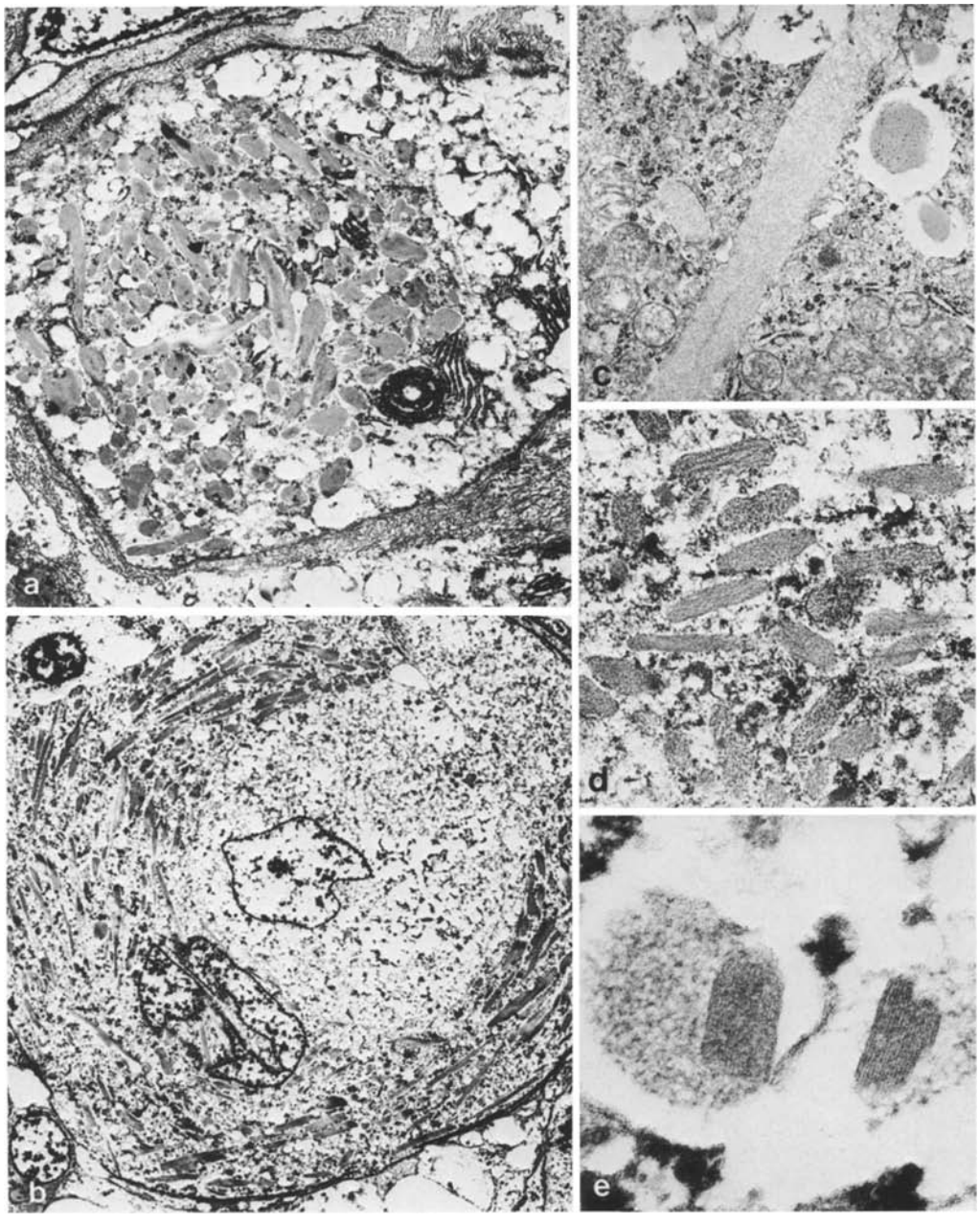

Fig. 6a and **b**. Tumor cells with numerous spicular and rhomboid crystals, in **b** with a tendency towards a concentric arrangement around the two nuclei. **c** Rod-shaped segment of dilated smooth ER filled with grey dense material. **d** and **e**. Crystals partly showing a distinct laminar structure. **a** ×5,360; **b** ×2,480; **c** ×15,100; **d** ×15,100; **e** ×78,800

ing characteristics resembling the cytoplasmic crystals, although they lacked the characteristic laminar structure of the crystals (Fig. 6c). The abundant, grouped mitochondria were generally round and of uniform size. Lipid droplets and glycogen deposits often intimately associated with each other (Fig. 5a) were common findings. Homogeneous dense granules of variable size and shape were seen in many tumor cells (Fig. 5d). There was a very sparse network of intermediate filaments throughout the cytoplasm. Bundle formations or thin cytofilaments of the actin type were not observed. In one case occasional tumor cells contained uniform, rounded virus-like bodies within the cytoplasm (Fig. 5b, inserted).

The amount, distribution, size and shape of the cytoplasmic crystals varied considerably from case to case and between different areas of the same tumor. In the seven cases where reprocessed paraffin-embedded material was used the distinct la-

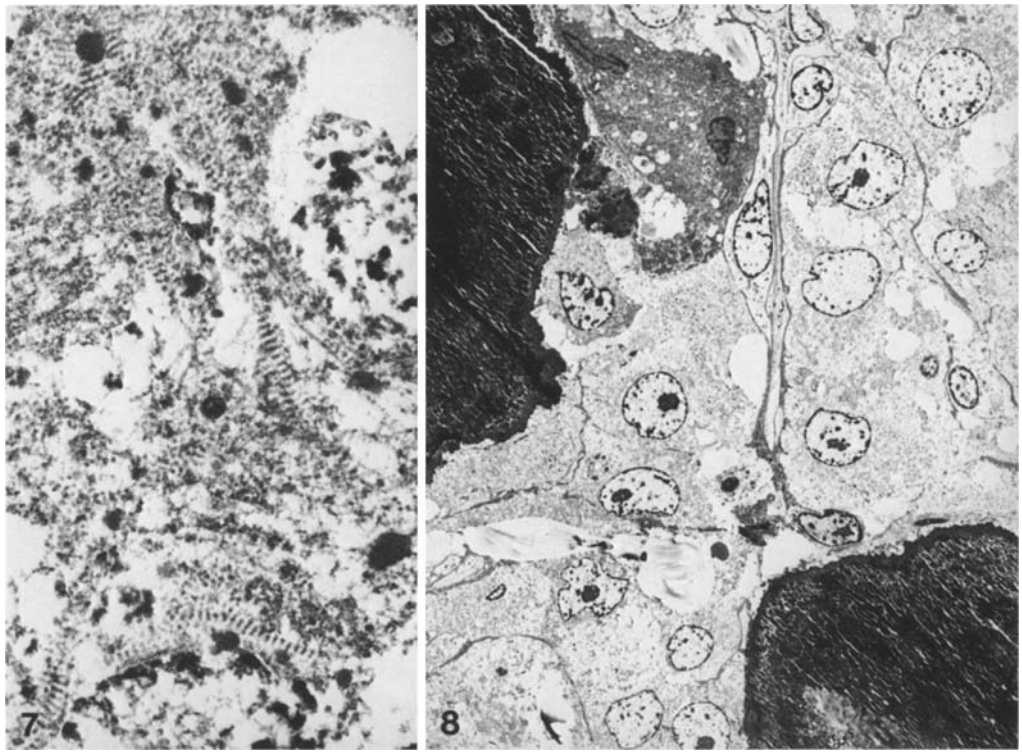

Fig. 7. Stroma containing collagen of the long-spaced type. ×12,100

Fig. 8. Tumor area with two psammoma bodies showing a peripheral dense zone in direct contact with the tumor cells and a multinucleated foreign body giant cell. ×8,600

minar structure, so prominent in the other three cases, was more or less destroyed, although they were easily recognized by their characteristic rhomboid, spicular or polyhedral shape (Figs. 6a, b, d, e). There were a few, desmosome-like, specialized contacts between the tumor cells. The external surface of the peripheral cells of the cell nests was covered by an external lamina (Fig. 5e) and occasionally segments of such lamina partly separated the closely packed individual tumor cells. The collagen of the stroma enclosing the cell nests had an ordinary appearance; in addition there were also fibers of the so-called long spaced type in two cases (Fig. 7). The prominent calcifications (case 1) were bordered by tumor cells in various stages of cell necrosis and revealed a distinct zonal composition with a peripheral, dense and homogeneous zone and a central granular core (Fig. 8).

Immunohystochemistry

The results of the immunohystochemical analysis of both control tissues and tumors are summarized in Table 3.

The tumor cells were negative for vimentin in all cases. There was a strong positivity of the fibroblasts and endothelium of the vascular stroma which enclosed the tumor cell nests and alveoli (Fig. 9a).

In eight of the ten tumors there were tumor cells positively stained for desmin. In most cases they appeared in scattered groups and the vast majority of the tumor cells were negative (Fig. 9b). In one of the negative cases the surrounding skeletal muscle and smooth muscle of vessels of venous type within the peripheral fibrous and vascular zone were also unstained as opposed to the other nine cases where these internal controls were intensely stained. In this case the tumor was fixed in sublimate solution.

Six of the ten tumors were positive for actin. Like desmin the majority of the tumor cells were negative and the positive tumor cells were usually found in scattered groups. In one case (case 10) a strong positivity was seen in a lung metastasis, while there was only slight positivity in the primary tumor.

There was no positive staining of the tumor cells for myoglobin, while the skeletal muscle showed a strong positivity.

All tumors were negative for the monoclonal anticytokeratin antibodies CAM 5.2 and AE1/

Table 3. Results of the immunohistochemical analysis of 10 cases of ASPS

Antigen	Controls		Tumors	
	Positive internal controls	Other positive controls (if no internal control)	Positive	Comments
Vimentin	Vascular endothelium, fibroblasts		0/10	Positivity in endothelium and fibroblasts of the vascular stroma
Desmin	Skeletal muscle, smooth muscle of veins		8/10	Focal groups of positive tumor cells
Actin	Vascular endothelium and muscle, fibroblasts, smooth muscle		6/10	Mostly scattered groups of positive tumor cells
Myoglobin	skeletal muscle		0/10	
Cytokeratins		Skin including epidermal appendages, squamous carcinoma, ductal breast carcinoma	0/10	In some cases positivity of tumor cells considered unspecific
EMA		Epidermal appendages, ductal breast carcinoma	0/10	
HMFG-1 and-2		Epidermal appendages, ductal breast carcinoma	0/10	
TPA		Epidermal appendages, breast carcinoma	0/10	
S-100 protein	Schwann cells of nerves		0/10	
Neurofilament			0/10	
Glial Fibrillary Acidic protein (GFAP)		Glial cells in teratoma of ovary	0/10	
Neuron specific enolase (NSE)		Ganglion cells of intestinal wall, carcinoid	10/10	A weak positivity was also seen in smooth muscle
F-VIII RAG	Vascular endothelium		0/10	
Laminin	External lamina of vessels		10/10	Positivity around the cell nests and alveoli; occasionally around individual tumor cells
Collagen IV			10/10	

AE3. The other monoclonal antibodies (PKK 1, 2080) produced some positivity in six cases and the polyclonal anticytokeratin antibodies (A575, Z622, 1084) in all cases. However, they also produced a similar staining of skeletal muscle, smooth muscle of veins, endothelium and fibroblasts, thus indicating an unspecific staining of structures other than cytokeratin. This non-specific staining was generally completely abolished as was the staining of tumor cells after pretreatment with trypsin. The control epithelial tissues were positively stained after pretreatment with trypsin as well.

No positivity was seen in the tumor cells for EMA, HMFG-1 and HMFG-2. There was a strong positivity in control tissues such as epidermal appendages and ductal breast carcinoma.

Tumor cells were negative for S-100-protein, while strong positivity was seen in Schwann cells of small nerves in the surrounding muscle tissue. No positivity for neurofilament was present in the tumor cells while the axons of small nerves were positively stained. There was no positive staining for glial fibrillary acidic protein. A positive staining was seen in glial cells of control tissue. Tumor cells were positively stained for neuron specific enolase in all cases. A positive staining was seen in ganglion cells of the intestinal wall and a weak positivity was seen in smooth muscle cells.

The tumor cells were negative for FVIII-RAG, while the endothelium of vessels was positively stained.

A strong positivity for Laminin and Collagen IV was seen along the outer borders of the tumor cell nests and alveoli and occasionally

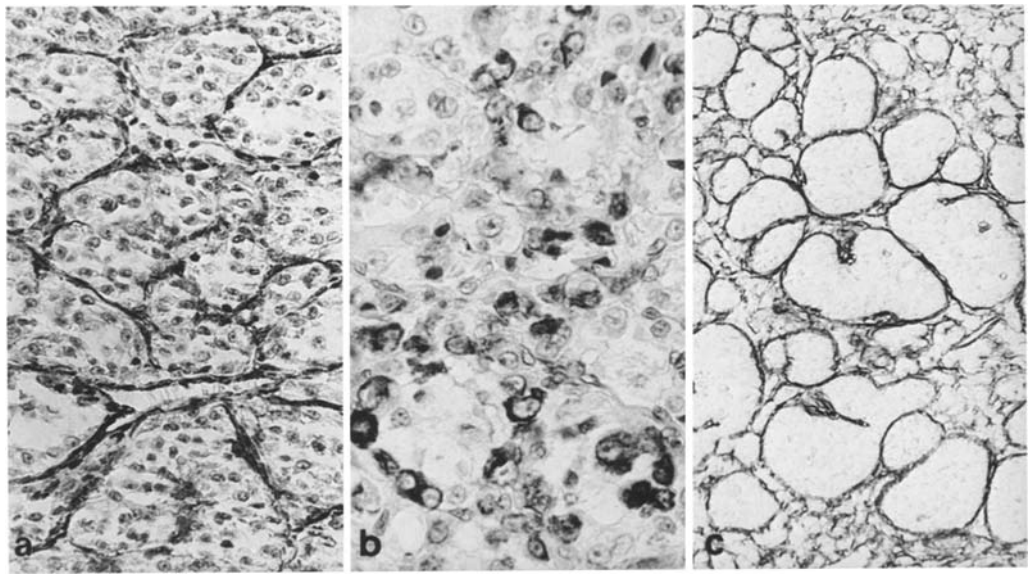

Fig. 9a. Fibroblasts and endothelium of the stroma are positively stained for vimentin, while the tumor cells are negative. **b** Area with scattered tumor cells positively stained for desmin. **c** The periphery of the alveoli and tumor cell nests and occasional single tumor cells are lined by material positively stained for laminin. (Avidin-biotin-complex method counterstained with hematoxylin). **a** ×160; **b** ×360; **c** ×160

around individual, mostly peripheral tumor cells. There was also a strong positive staining around the vascular spaces in the septa which divided the cells nests and alveolar structures (Fig. 9c).

DNA-analysis

Figure 10 illustrates and Table 4 describes histograms based on scanning microspectrophotometric measurements of nuclear DNA measured in paraffin sections in ten ASPS. All ASPS have a modal DNA peak in the diploid range. The analysis of the ASPS of the ordinary type having a diploid DNA-peak indicated, with one exception (case 8) low cell proliferation – less than a third of their nuclei exceeded the diploid values as well as 2.5 c and the 90th percentile of the DNA values of the control cells. Two of the tumors were wholly or partly of the pleomorphic variant (cases 10 and 3) and these had an additional non-diploid peak between 3c and 4c and a high proportion of cells exceeding the diploid value as well as 2.5c and 90th percentile of the control cells. The tumors not only showed a variation in DNA content among each other corresponding to differences in their histopathological presentation but also showed regional variations within the same tumor as in case 8. In this case measurements, when restricted to a small pleomorphic area showed a tetraploid peak, which was not registered when nuclear DNA was measured randomly (Fig. 11). Even in the wholly pleomorphic ASPS histograms of the most pleomorphic areas showed a broader distribution of DNA values among the tumor cells and the occurrence of higher amounts of nuclear DNA than in less pleomorphic areas (Fig. 11). DNA-histograms of the primary tumor and of the lung-metastases of case 10 were all polyploid – the primary tumor containing higher proportions of polyploid nuclei (Fig. 12).

By measurements of nuclei of aspirated tumor cells in smears from one of the pleomorphic ASPS (case 10) the abnormal peak of 3.3 c in section could be identified as tetraploid (4c) (Fig. 13). The DNA values between 3c and 4c in the other ASPS shown in Fig. 8 probably also represents tetraploid nuclei.

Discussion

All ten cases in this series had a light-microscopic appearance characteristic of alveolar soft part sarcoma (ASPS). However, one of them differed by presenting a prominent nuclear polymorphism throughout and two other by showing some polymorphic areas. In 1952 Christopherson et al. described polymorphic areas in one tumor in their series of ASPS. We know of only one case of ASPS from the literature which has been described as a pleomorphic variant (Evans 1985). A fourth tumor showed areas with calcification of the psammoma body type; to our knowledge this has not been previously described in ASPS.

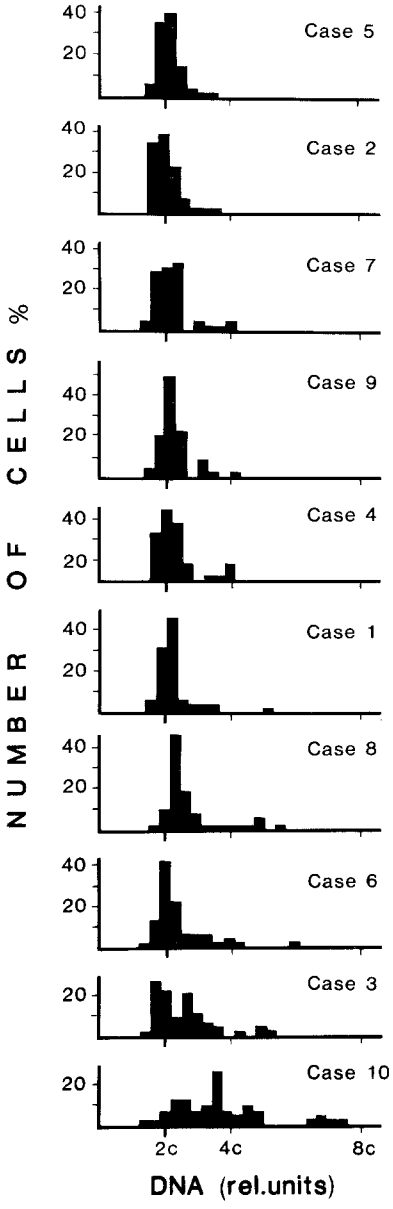

Fig. 10. DNA-histograms of 10 cases of alveolar soft part sarcoma according to the increasing percentage of cells exceeding the modal value

Table 4. Description of histograms

Case number	Modal DNA value relative units	Percentage of cells exceedings		
		Modal value	2.5 c of control cells	P_{90} of control cells
5	2.0	4	15	18
2	2.0	6	17	16
7	2.0	10	12	22
9	2.0	12	12	22
4	2.0	12	19	22
1	2.0	17	17	20
8	2.36	18	46	44
6	2.0	25	27	28
3	1.81	46	47	46
10	2.46	70	78	80

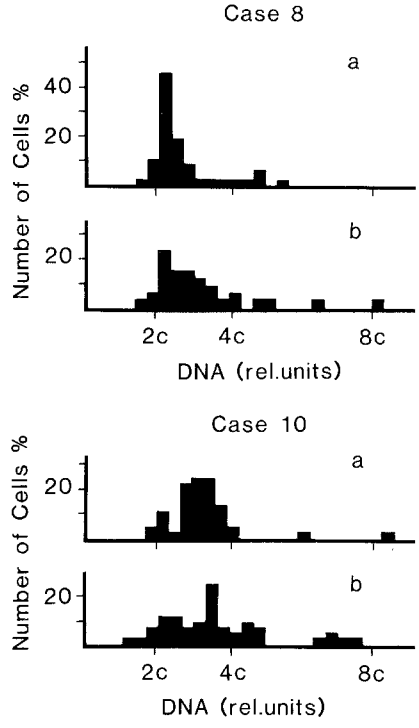

Fig. 11. Regional variation in DNA content of the same tumor. In case 8 measured areas of ordinary appearance are marked a, while pleomorphic areas are marked b. In case 10, which is of the pleomorphic type throughout, areas with less polymorphism are illustrated in a, while prominent polymorphism is illustrated in b

Experience of the cytologic appearance of ASPS is restricted to a single report of a case where imprints were described (Uehara 1978) and an illustration of our cytologically studied case in an atlas (Orell et al. 1986). The epithelial features of the tumor cells obviously make it difficult to distinguish ASPS from a carcinoma, especially renal cell carcinoma, in the smears. We feel that it may also be difficult to decide from smears whether the ordinary type of ASPS is a benign or malignant tumor. The single case studied in our series was of the pleomorphic variant and the cytologic examination showed prominent polymorphism which clearly indicated a malignant tumor, although the type could not be determined.

The finding of desmin positive tumor cells in 8 of 10 cases is in accordance with the demonstration of desmin by Mukai et al. (1986) in their three cases, using a polyclonal antibody. Denk et al. (1983) also found desmin in their immunofluorescence study of a case of ASPS using another poly-

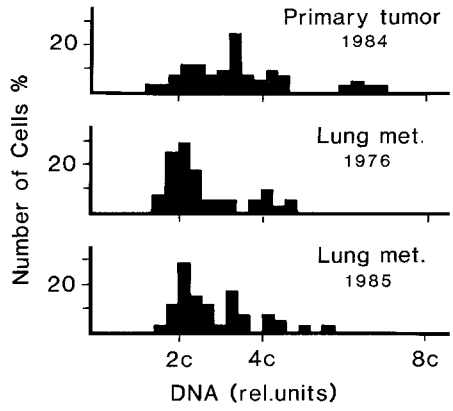

Fig. 12. Histograms of the primary tumor and lung metastases of a pleomorphic variant of alveolar soft part sarcoma (case 10) showing a bimodal, di-tetraploid pattern, which is more pronounced in the primary tumor

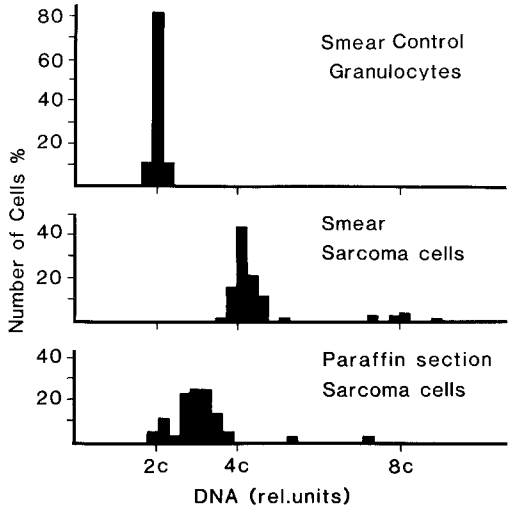

Fig. 13. Smears of pleomorphic ASPS (case 10) containing tetraploid tumor cell as compared to control granulocytes. Paraffin sections of the same tumor show that the tetraploid (4 c) peak has shifted to a falsely low modal value of 3.3 c

clonal antibody. Our findings, however, differ from these two studies in terms of vimentin positivity. In our series the tumor cells were negative for vimentin in all cases, in contrast to the strong positivity of fibroblasts and of endothelium of the vascular septa dividing the tumor cell nests. In our hands the monoclonal vimentin antibody used in the present study has proved useful and reliable without unspecific staining or cross-reactivity with other types of intermediate filaments. However, we have found that the monoclonal antibody used by Mukai et al. also gives a positivity to mature skeletal muscle and some epithelial structures, thus suggesting a cross-reactivity with other classes of intermediate filaments, when formalin-fixed and paraffin-embedded tissues are used.

The positive staining of the tumor cells obtained by the three polyclonal and two of the monoclonal anticytokeratin antibodies used is probably non-specific, since positivity was also found in other cells, such as fibroblasts, endothelium and skeletal muscle. Moreover, this positivity was completely abolished by pretreatment with trypsin in most cases and there was no positivity for cytokeratin using the monoclonal CAM 5.2 and AE1/AE3 anticytokeratin antibodies, which in our hands have been found most reliable. A negative staining for cytokeratin was also noted by Mukai et al. (1986).

Ultrastructurally a sparse network of intermediate filaments was found, which many represent desmin. The sparseness of intermediate filaments seen ultrastructurally contrasts with the strong desmin positivity seen immunohistochemically. However, such desmin-positive cells only appeared in scattered areas. Consequently such cells may not have been included in the tissue pieces examined ultrastructurally. The absence of intermediate filament bundles and tonofilament structures is in agreement with our interpretation of the immunohistochemical results of cytokeratins as being negative. There were no other ultrastructural features indicating an epithelial differentiation either. Moreover, the results of the studies of other markers for epithelial differentiation, EMA, HMFG 1 and 2 and TPA, were also negative.

The results of our ultrastructural and immunohistochemical studies did not support the hypothesis of neural crest origin of ASPS (Mathew 1982). The dense granules seen in some tumor cells clearly differ from neurosecretory granules as described in paraganglioma (Lack et al. 1979). Myelin sheaths or myelinated axons as previously described in a case of ASPS (Mathew 1982) were not found in our series. Mukai et al. (1983) also failed to find any myelin membrane proteins (P0, P2) in their immunohistochemical analysis. The presence of long-spaced collagen, as seen in two of our cases and previously reported in another case (Mathew 1982), is by no means specific for nerve sheath tumors (Henderson et al. 1986). Moreover, there was no positivity for S-100 protein, GFAP or neurofilaments. Similar results was found by Mukai et al. (1983; 1986). The negativity for S-100 protein militates against neuroectodermal origin.

From the results of a correlative light and electron microscopic study of granular cell tumor, malignant melanoma, carotid body paragang-

lioma, alveolar rhabdomyosarcoma, nemaline myopathy and a case of ASPS, Fisher and Reidbord (1971) suggested a myogenic derivation of ASPS; they also suggested that it represents a unique type of rhabdomyosarcoma. This conclusion was then mainly based on the striking morphological similarity between the crystalline rods of ASPS and the nemaline-body-like rods seen in their cases of nemaline myopathy, and in alveolar rhabdomyosarcoma, and also described in adult rhabdomyoma (Enzinger and Weiss 1983). The nemaline-body-like rods seen in adult rhabdomyosarcoma and occasionally in alveolar rhabdomyosarcoma appear to be derived from abnormal hypertrophic Z-bands (Price et al. 1965). Z-bands are known to contain desmin and actin as well as α-actinin and tropomyosin (Mukai et al. 1983). In the recent study of Mukai et al. (1986) Z-protein was demonstrated in ASPS, thus indicating a skeletal muscle differentiation. The abundance of cytoplasmic glycogen seen in our series of ASPS is also a characteristic finding of the tumor cells of rhabdomyoma and differentiated rhabdomyoblasts of rhabdomyosarcoma (Seidal and Kindblom 1984). Moreover, such myogenic tumor cells form external lamina material (Seidal and Kindblom 1984) as seen in peripheral parts of the tumor cell nests of ASPS. The presence of external lamina material was shown to be even more prominent by the immunohistochemical staining for collagen IV and laminin. Similar staining patterns for collagen IV and laminin have been described in alveolar rhabdomyosarcoma (Autio-Harmainen et al. 1986). The age and anatomic distribution of ASPS also suggests a relationship with rhabdomyosarcoma. ASPS in children often involves the head and neck region, which are also common locations for embryonal and alveolar rhabdomyosarcoma. Rhabdomyoma of adult type, like ASPS, shows a predilection for the tongue. In contrast to rhabdomyosarcoma and adult rhabdomyoma, however, ASPS was negative for myoglobin and lacked bundles of thin and thick myofilaments with Z-band-like condensations ultrastructurally. On the other hand, desmin positivity and vimentin negativity, as seen in this series of ASPS, is also found in adult rhabdomyoma and in the differentiated rhabdomyoblasts of rhabdomyosarcoma (Seidal et al. 1987). The controls of the polyclonal anti-NSE antibody used here indicate that it is not entirely specific to cells of neuroectodermal origin since smooth muscle cells were partly positively stained by the antibody. When it comes to the possible rhabdomyoblastic differentiation of ASPS, it is interesting to note that NSE-positivity has previously been described by Tsokos et al. (1984) in differentiated rhabdomyoblasts of embryonal rhabdomyosarcoma using another polyclonal antibody.

The nature and origin of the crystalline rods of ASPS has been debated and, following a digital image processing analysis, Mukai et al. (1986) have, suggested that they represent actin filaments. Others have suggested a lysosomal origin (Kamei et al. 1984), a relation to the small dense granules seen in many tumor cells (Ekfors et al. 1979) and to the renin granules of the juxtaglomerular cells (DeSchryver-Kecskemeti et al. 1982). The rod-shaped dilated segments of endoplasmic reticulum filled with dense material seen in this series might represent an early stage of the crystal formation, suggesting that the material for the formation of the crystals is produced and at least partly organized within the endoplasmic reticulum.

No systematic studies of the relationship between the histopathologic type of soft tissue sarcoma and DNA content, or of the significance of ploidy with respect to prognosis, have been published. In general, benign soft tissue tumors have shown a normal DNA content and a diploid DNA distribution, while especially high grade sarcomas have been found to be aneuploid (Kreicbergs et al. 1987). Among high grade sarcomas, however, some tumors have also been found to be diploid, especially monomorphic sarcomas such as the monophasic type of synovial sarcoma. It is interesting to note that many ASPS and synovial sarcomas have a diploid DNA distribution and a prolonged course in common.

In ASPS there is an obvious parallel between the histopathologic picture and the DNA histogram pattern in that all the ASPS of the ordinary type (7/10) were diploid, while the three which were wholly or partly of the pleomorphic type had a diploid and tetraploid peak. Cytochemical determinations of the DNA content thus permit characterization of ASPS as euploid. Furthermore, the pleomorphic tumors did not differ in mitotic activity from the other cases and there was no difference in clinical behavior between the seven diploid and the three diploid-tetraploid ASPS. The occurrence of tetraploidy in the pleomorphic cases could mean that these tumors had started to proliferate and change their DNA content from diploid to tetraploid. This is however contradicted by the polymorphic appearance and the bimodal diploid-tetraploid DNA content of the lung metastasis of case 10 as early as eight years before the primary tumor was discovered. Whatever the cause of the polyploidy it seems likely that differences in DNA distribution in this type of tumor are related to

the nuclear size and polymorphism rather than its aggressiveness.

In summary our investigation gives support to the hypothesis of a rhabdomyoblastic differentiation, although ASPS present features clearly distinguishing them from rhabdomyosarcoma. It is possible that ASPS represent a specific variant of rhabdomyoblastic sarcoma, with an euploid DNA distribution, where the tumor cells have maintained properties of muscle cells and differentiated rhabdomyoblasts, such as the expression of desmin, the lack of vimentin, the production of external lamina material and crystals resembling Z-band material, although the cells lack the ability to form myoglobin and myofilament bundles.

Addendum

Since the submission of this paper a series of ASPS has been described by Auerbach and Brooks (Cancer 60:66–73, 1987) along with an immunohistochemical analysis of 9 cases. Contrary to our findings of a positivity for desmin in 8 of 10 cases, all of their 9 tumors were reported to be negative for desmin. When now completing this study with the monoclonal anti-desmin antibody used by Auerbach and Brooks we did not find any positivity in our 10 tumors either. However, we have found the three polyclonal and the single monoclonal anti-desmin antibodies used in their analysis inferior in the diagnosis of rhabdomyoblastic tumors, compared to the monoclonal anti-desmin antibody in this study, when using formalin-fixed and paraffin-embedded tissues (Seidal T, Kindblom L-G, Angervall L: Myoglobin, desmin and vimentin in ultrastructurally proven rhabdomyomas and rhabdomyosarcomas. An immunohistochemical study utilizing a series of monoclonal and polyclonal antibodies. Appl. Pathol. 5:201–209, 1987). The reported negativity for desmin in Aurbach's and Brooks' series, which is in contrast to our and Mukai's (1986) findings, can therefore probably be explained by different properties of the antibodies used.

References

Altmannsberger M, Dirk T, Osborn M, Weber K (1986) Immunohistochemistry of cytoskeletal filaments in the diagnosis of soft tissue tumors. Semin Diagnostic Pathol 4(3):306–316

Autio-Harmainen H, Apaja-Sarkinnen M, Martikainen J, Taipale A, Rapola J (1986) Production of basement membrane laminin and type IV collagen by tumors of striated muscle: An immunohistochemical study of rhabdomyosarcomas of different histologic types and a benign vaginal rhabdomyoma. Hum Pathol 17:1218–1224

Caspersson T (1979) Quantitative tumor cytochemistry. C H A Clowes Memorial Lecture. Cancer Res 39:2341–2355

Caspersson T, Kudynovski J (1980) Cytochemical instrumentation for cytopathological work. Int Rev Exp Pathol 21:1–54

Chaundry AP, Lin CC, Lai S, Yamane G (1984) Alveolar soft part sarcoma of the tongue in a female neonate. J Oral Med 39(1):2–7

Christopherson WM, Foote FW, Stewart FW (1952) Alveolar soft-part sarcomas. Structurally characteristic tumors of uncertain histogenesis. Cancer 5:100–111

Denk H, Krepler R, Artlieb U, Gabbiani G, Rungger-Brändle E, Leoncini P, Franke WW (1983) Proteins of intermediate filaments. An immunohistochemical and biochemical approach to the classification of soft tissue tumors. Am J Pathol 110:193–208

DeSchryver-Kecskemeti K, Kraus FT, Engleman W, Lacy PE (1982) Alveolar soft-part sarcoma – A malignant angioreninoma. Histochemical, immunocytochemical, and electron-microscopic study of four cases. Am J Surg Pathol 6:5–18

Ekfors TO, Kalimo H, Rantakokko V, Latvala M, Parvinen M (1979) Alveolar soft part sarcoma. A report of two cases with some histochemical and ultrastructural observations. Cancer 43:1672–1677

Enzinger FM, Weiss SW (1983) Soft tissue tumors. Mosby, St Louis

Evans HL (1985) Alveolar soft-part sarcoma. A study of 13 typical examples and one with a histologically atypical component. Cancer 55:912–917

Fisher ER (1956) Histochemical observations on an alveolar soft-part sarcoma with reference to histogenesis. Am J Pathol 32:721–737

Fischer ER, Reidbord H (1971) Electron microscopic evidence suggesting the myogenous derivation of the so-called alveolar soft part sarcoma. Cancer 27:150–159

Font RL, Jurco S, Zimmerman LE (1982) Alveolar soft-part sarcoma of the orbit: A clinicopathologic analysis of seventeen cases and a review of the literature. Hum Pathol 13:569–579

Gray GF, Glick AD, Kurtin PJ, Jones HW (1986) Alveolar soft part sarcoma of the uterus. Hum Pathol 17:297–300

Henderson DW, Papadimitriou JM, Coleman M (1986) Ultrastructural appearances of tumors. Diagnosis and classification of human neoplasia by electron microscopy. Second edition. Churchill Livingstone, London

Hsu SM, Raine L, Fanger H (1981) Use of avidin-biotin-peroxidase complex (ABC) in immunoperoxidase techniques: A comparison between ABC and unlabeled antibody (PAD) procedures. J Histochem Cytochem 29:577–580

Kamei T, Ishihara T, Yamashita Y, Takahaski M, Uchino F, Ishizaka H, Moroki Z, Ueda N (1984) An ultrastructural and histochemical study of alveolar soft part sarcoma with special reference to the nature of crystals. Acta Pathol Jpn 34:435–443

Komori A, Takeda Y, Kakiichi T (1984) Alveolar soft-part sarcoma of the tongue. Report of a case with electron microscopic study. Oral Surg 57:532–539

Kreicbergs A, Tribukait B, Willems J, Bauer HCF (1987) DNA flow analysis of soft tissue tumors. Cancer 59:128–133

Lack EE, Cubilla AL, Woodruff JM (1979) Paragangliomas of the head and neck region. A pathologic study of tumors from 71 patients. Hum Pathol 10:191–218

Mathew T (1982) Evidence supporting neural crest origin of an alveolar soft part sarcoma. Cancer 50:507–514

Mukai M, Iri H, Nakajima T, Hirose S, Torikata C, Kageyama K, Ueno N, Murakami K (1983) Alveolar soft-part sarcoma. A review on its histogenesis and further studies based

on electron microscopy, immunohistochemistry och biochemistry. Am J Surg Pathol 7:679–689

Mukai M, Torikata C, Iri H, Mikata A, Sakamoto T, Hanaoka M, Shinohar C, Baba W, Kanaya K, Kageyama K (1984) Alveolar soft part sarcoma. An elaboration of a three-dimensional configuration of the crystalloids by digital image processing. Am J Pathol 116:398–406

Mukai M, Torikata C, Iri H, Mikata A, Hanaoka H, Kato K, Kageyama K (1986) Histogenesis of alveolar soft part sarcoma. An immunohistochemical and biochemical study. Am J Surg Pathol 10(3):212–218

Orell SR, Sterrett GF, Walters MNI, Whitaker D (1986) Manual and atlas of fine-needle aspiration cytology. Churchill Livingstone, London

Price HM, Gordon GB, Pearson CM, Munsat TL, Blumberg JM (1965) New evidence for excessive accumulation of Z-band material in nemaline myopathy. Proc Natl Acad Sci USA 54:1398–1406

Romdhane KB, Lacombe MJ, Boddaert A, Bertin F, Genin J, Rouesse J, Contesso G (1985) Les sarcomes alvéolaires des parties molles. A propos de 6 cas et revue de la littérature. Ann Pathol 5(3):159–166

Seidal T, Kindblom LG (1984) The ultrastructure of alveolar and embryonal rhabdomyosarcoma. A comparative light and electron microscopic study of 17 cases. Acta Pathol Microbiol Immunol Scand [Suppl] 92:231–248

Seidal T, Kindblom LG, Angervall L (1987) Myoglobin, desmin and vimentin in ultrastructurally proven rhabdomyomas and rhabdomyosarcomas. An immunohistochemical study utilizing a series of monoclonal and polyclonal antibodies. Appl Pathol 5:201–209

Shipkey FH, Lieberman PH, Foote FW, Stewart FW (1964) Ultrastructure of alveolar soft part sarcoma. Cancer 17(7):821–830

Tsokos M, Linnoila RI, Chandra RS, Triche TJ (1984) Neuron specific enolase in the diagnoses of neuroblastoma and other small, round-cell tumors in children. Hum Pathol 15:575–584

Uehara H (1978) Cytology of alveolar soft part sarcoma. Acta Cytol 22(4):191–192

Unni KK, Soule EH (1975) Alveolar soft part sarcoma. An electron microscopical study. Mayo Clin Proc 50:591–598

Wang S, Mirra J, Bhuta S (1984) Alveolar soft part sarcoma following radiotherapy for a spinal hemangioma. A case report. Cancer 53:2655–2660

Welsh RA, Bray DM, Shipkey FH, Meyer AT (1972) Histogenesis of alveolar soft part sarcoma. Cancer 29:191–204

Widéhn S, Kindblom LG (1988) A rapid and simple method for diagnostic electron microscopy of paraffin-embedded tissue Ultrastruct Path 12(1)

Accepted January 4, 1988